Journal of Thermoplastic Composite Materials OnlineFirst, published on June 30, 2009 as doi:10.1177/0892705709099694

Polypropylene Nanocomposites with Thermally Stable Imidazolium Modified Clay: Mechanical Modeling and Effect of Compatibilizer

V. MITTAL*,**

Department of Chemistry and Applied Biosciences, Institute of Chemical and Bioengineering, ETH Zurich, 8093 Zurich, Switzerland

ABSTRACT: Thermally stable imidazolium modification as compared to the conventional ammonium modification is chosen to prepare polypropylene nanocomposites. Different volume fractions of organo-montmorillonite are used to generate polymer nanocomposites and the effect of the modified clay on mechanical properties is studied. The mechanical properties are also compared with Halpin–Tsai models and its modified versions to achieve better insight into the system. Addition of small amount of compatibilizer enhanced the extent of delamination of the filler. Compatibilizers are selected on the basis of their chemical nature, molecular weight, amount of grafting, and location of the polar groups. Incompatibility of the surface modification with the compatibilizer is suspected to counterbalance the delamination effect thus resulting in no change or deterioration of the oxygen permeation through the composite films. However, the tensile modulus is enhanced on addition of comaptibilizer owing to increased exfoliation, which exceeded the amount of matrix plasticization caused by the addition of the low-molecular weight compatibilizer. The compatibilizers neither affected the crystallization behavior of polymer nor the thermal behavior of the resulting composite.

KEY WORDS: polypropylene, imidazolium modified montmorillonite, mechanical properties, gas permeation, mechanical modeling.

INTRODUCTION

LAYERED SILICATE NANOCOMPOSITES, in which at least one dimension of the filler is in the range of 100 nm, have revolutionized the research

*E-mail: vikas.mittal@chem.ethz.ch
**Present address: BASF SE, Polymer Research, Ludwigshafen, Germany.

0892-7057/08/00 0001–22 $10.00/0 DOI: 10.1177/0892705708099694

in composite materials owing to the significant enhancement of the properties at very low filler volume fractions [1–6]. Aluminosilicates, especially montmorillonite, has received significant attention as the inorganic filler to prepare these nanocomposites owing to their easy swelling in water leading to 1 nm thick platelets [7,8]. This leads to easy exchange of alkali metal cations present on the surface of the platelets with long chain alkyl ammonium cations thus reducing the surface energy and making the treated montmorillonite more compatible in the polymer matrix leading to its nanoscale dispersion [9,10]. This synergism is then translated into the enhanced properties like mechanical and barrier performance, heat deflection temperature, ablation and flammability resistance etc. [1–6].

Polypropylene (PP) is a material of choice for a number of applications. The pure polymer is often compounded with surface modified inorganic fillers to further enhance its properties [11–13] by following the common melt intercalation approach. However, significantly higher temperatures in the range of 200°C are required for melt intercalation process and the organic ammonium modifications have been observed to have onset of degradation as low as 180°C by TGA studies [14]. The thermal degradation follows Hoffmann degradation path involving the early breakage of weaker C–N bond in the ammonium modification. The thermodynamics of the system and the resulting interfacial interactions can be affected even with the rupture of a small number of bonds [15–19]. Many approaches have been tried to circumvent this limitation of thermal stability of the ammonium cations attached to the clay surface [20–22], out of which the use of other thermally stable cations such as phosphonium, pyridinium, and imidazolium offers a good alternative to the ammonium salts [23,24]. Thermal studies carried out especially on imidazolium salts have proved their much better thermal response as compared to the alkyl ammonium cations both in the presence and absence of oxygen as degrading atmosphere [23]. However, the use of such salts for the synthesis of polymer nanocomposites needs to be expanded.

The interplay of enthalpic and entropic forces governs the generation of final morphology in the nanocomposites. In PP-filler system, strong enthalpic interactions between the surface modified filler and PP chains are absent, therefore, it leads to only a limited development, at best partial exfoliation. In order to compatibilize both the organic polymer and inorganic filler phases, polypropylene-graft-maleic anhydride (PP-g-MA) has been commonly used as amphiphilic compatibilizer or non-ionic surfactant [25–31]. Effect of molecular weight of PP-g-MA, amount of PP-g-MA and extent of grafting of MA on morphology, filler exfoliation, and resulting composite properties has been extensively studied. Higher extents of filler exfoliation have been reported when amount of PP-g-MA with respect to organically modified montmorillonite (OMMT) was increased, but an optimum amount of grafting was required to achieve better mixing as higher grafting can also create immiscibility with the polymer matrix [25–27]. The mechanical properties also enhanced with the amount of PP-g-MA, but after a certain weight percent of PP-g-MA, a decrease in the properties was also observed [32,33]. It is also of interest to study the behavior of block copolymers with PP as these copolymers have been reported to have better performance than the grafted counterparts [34].

The mechanical behavior of particulate composites has been explained by using a number of micro-mechanical models developed over the years [35–38]. Halpin–Tsai model has received special attention owing to better prediction of the properties for a variety of reinforcement geometries. The η values in the model is given by the expression

$$\eta = \frac{(E_f E_m - 1)}{(E_f / E_m + \zeta)}$$

where E_f is the modulus of the filler and E_m is the modulus of the pure polymer matrix. ζ represents the shape factor, which is dependent on filler geometry and loading direction. For the composites containing oriented discontinuous ribbon or lamellae, η is estimated to be twice the aspect ratio. It has been reported to over-predict the stiffness in this case; therefore, its value was reported to be 2/3 times the aspect ratio [39]. However, other assumptions in the models like firm bonding of filler and matrix, perfect alignment of the platelets in the matrix, uniform shape, and size of the filler particles in the matrix make it very difficult to correctly predict the nanocomposites properties. The model has recently been modified in order to accommodate the effect of incomplete exfoliation and misorientation of the filler, but the effect of imperfect adhesion at the surface still needs to be incorporated [40,41].

The goal of the present investigation was to study the PP nanocomposites synthesized with thermally stable imidazolium treated montmorillonite. The mechanical properties of these nanocomposites were modeled using a number of micro-mechanical models. The effect of compatibilizers with different architecture on mechanical and oxygen permeation properties of the OMMT-PP nanocomposites was studied. PP-g-MA of two different molecular weights and grafting amounts were used along with a PP-b-PPG. The surface modification of the filler and filler volume fraction were always kept the same to achieve quantitative comparisons.

EXPERIMENTAL

Materials

PP used was the homopolymer grade H733-07 from Dow (Dow Plastics, Horgen, Switzerland). It has a melt flow index of 7.5 g/10 min (230°C at 2.16 kg load) and a density of 0.9 g/cm^3. Sodium montmorillonite with a trade name of Cloisite Na was purchased from Southern Clay Inc. (Gonzales, Texas, USA). The cation exchange capacity (CEC) of the sodium montmorillonite was determined to be 880 μeq/g by exchanging its sodium ions with Cu(trien)$^{2+}$ [42]. 1-Decyl-2-methyl-3-octadecylimidazolium bromide was synthesized as reported earlier [43]. Two different kinds of compatibilizers were used: PP-g-MA1 with a trade name of Admer QF551E was supplied by Alcan Packaging (Neuhausen, Switzerland), whereas PP-g-MA2 was procured from Aldrich (Buchs, Switzerland). Block copolymer PP-b-PPG was synthesized as described in an earlier study [44].

Filler Surface Modification and Composite Preparation

The exchange of the imidazolium salt on the montmorillonite surface was carried out by the process reported earlier [43]. Both degree of exchange and the purity of the product were monitored by Hi-Res TGA. Subsequently, the modified clay (OMMT) was suspended in dioxane, sonicated and freeze dried. The freeze dried clay was sieved (60 μm mesh) to obtain the fine OMMT powder. The required amounts of OMMT and polymer were calculated on the basis of desired inorganic volume fraction as reported earlier using the equation [45]:

$$M_{\mathrm{OMMT}} = M_{\mathrm{M}} + (M_{\mathrm{M}} * \mathrm{CEC} * M_{\mathrm{OC}})$$

$$M_{\mathrm{P}} = \left(\frac{M_{\mathrm{M}} * V_{\mathrm{P}} * \rho_{\mathrm{P}}}{V_{\mathrm{M}} * \rho_{\mathrm{M}}}\right) - (M_{\mathrm{M}} * \mathrm{CEC} * M_{\mathrm{OC}})$$

where M_{OMMT} is the mass of the OMMT, M_{M} is the mass of the inorganic aluminosilicate, M_{OC} is the molar mass of the organic ammonium cation used to modify the montmorillonite surface, M_{P} is the mass of PP, V_{M} is the inorganic volume fraction, ρ_{M} is the density of sodium montmorillonite (2.6 g/cm^3), V_{P} is the PP volume fraction and ρ_{P} is its density. Twin blade compounder (Plasticorder W 50 EH, Brabender, Duisburg, Germany) was used to prepare OMMT–PP composites. The polymer granules were molten at 190°C at 40 rpm, filler was then gradually added in 10 min at 50 rpm and the mixture was kneaded for further 10 min at 60 rpm. Thick plates of 1.5 mm were then compression molded in a brass frame between two thin aluminum plates [46]. Similarly, thin films (~100 μm) of the composites as well as pure PP were pressed by compression molding.

Characterization of Nanocomposites

Dumbbell shaped samples (type 5B) were stamped out of the compression molded nanocomposite and pure polymer plates using a stamping press (H. W. Wallace, Croydon, Surrey, England) with a die conforming to the standard ISO 527-2. Tensile tests on the stamped samples were carried out (ISO 527-1) at room temperature using a Zwick Z020 universal testing machine with testXpert 9.01 software (Zwick, Ulm, Germany) coupled with a Video-Extensometer V4.19.02 (Messphysik, Furstenfeld, Austria) for accurate measurement. The drawing speed of 0.1 mm/min was used for the measurement of elastic modulus and modulus was determined in the range of 0.05–0.25% strain. A speed of 6 mm/min was used for the measurement of other tensile properties and an average of five measurements was taken.

DSC 7 (Perkin Elmer, Norwark, CT) was used to carry out differential scanning calorimetric measurements at a heating rate of 10°C/min, adopting the procedure for measuring heat capacities [47]. A temperature range (100–180°C) was used to calculate the melting enthalpies of the composite samples followed by necessary corrections to represent the thermal behavior of pure PP in the composites. The experiments were repeated twice and an average value was reported.

High-resolution (Hi-Res) thermogravimetric analysis (TGA) of OMMT and composites, in which the heating rate is coupled to mass loss, that is, the sample temperature is not raised until the mass loss at a particular temperature is completed, was performed on a Q500 thermogravimetric analyzer (TA Instruments, New Castle, DE). All measurements were carried out in air in the temperature range 50–900°C at a heating rate of 20°C/min.

X-ray diffraction patterns were collected on a wide angle Scintag XDS 2000 diffractometer (Scintag Inc., Cupertino, CA) using Cu Kα radiation ($\lambda = 0.15406$ nm) in reflection mode. An average of three diffraction experiments was reported. Surface morphology of the fracture face of the nanocomposite material was obtained by immersing thick nanocomposites plaques in liquid nitrogen and instantly fracturing them. The surfaces of the compound were then sputter coated with 5 nm platinum and the morphology was observed in Hitachi S-900 field emission scanning electron microscope at an accelerating voltage of 15 kV. Bright-field TEM of the nanocomposites was performed with Zeiss EM 912 Omega microscope. Thin nanocomposite films were etched with oxygen plasma for 5 min and embedded in an epoxy matrix followed by sectioning of 70–90 nm thick sections subsequent supporting on 100 mesh grids sputter coated with a 3 nm thick carbon layer. OX-TRAN 2/20 ML (Mocon, Minneapolis, MN) modules at 23°C and 0% RH were used to measure oxygen permeation through these films [45]. An average of five values was reported.

RESULTS AND DISCUSSION

Dialkyl imidazolium treated montmorillonite was reported to be much more thermally stable than the conventional dimethyldioctadecylammonium modified counterpart [43]. The onset of degradation of imidazolium modified montmorillonite was delayed by around 50°C as compared to the ammonium treatment. Apart from the delayed onset of degradation in the imidazolium treated clay, the peak degradation temperature also was higher by almost 35°C. The dynamic TGA also showed faster thermal degradation in the ammonium treatment than the imidazolium counterpart. Furthermore, the compounding temperatures were kept low in order not to degrade the modification and the polymer, but high enough to ensure homogenous mixing. Along with the thermally stable head group, the long octadecyl chains in the surface modification also helps in significantly separating the clay platelets thus reducing the attractive forces among them and their similar chemical nature as PP is also expected to help in better intermixing at the interface. The surface treatment consisted of alkyl chains of two different lengths to avoid its possible phase separation at the interface with the polymer which sometimes have been reported for dimethyldioctadecylammonium modification owing to its more ordered structure [48].

Table 1 shows the basal plane spacing values of the filler in the OMMT- PP composites. The 001 peak of the modified filler was observed at 2.24 nm. It is clear from the basal plane spacing values of the filler in the nanocomposites

Table 1. d-spacing and tensile properties of OMMT–PP nanocomposites as a function of filler volume fraction.

Filler volume fraction	*d*-spacing	Tensile modulus[a] (MPa)	Yield stress[b] (MPa)	Yield strain[c] (%)	Stress at break[d] (MPa)
0.00	–	1510	36	9.4	29
0.01	2.52	1668	31	8.5	23
0.02	2.28	1810	28	6.0	22
0.03	2.29	1918	26	4.4	23
0.04	2.24	2007	24	3.9	21

Notes: [a]Relative probable error 5%.
[b]Relative probable error 2%.
[c]Relative probable error 5%.
[d]Relative probable error 15%.

that no extensive intercalation has taken place. Apart from that, a decrease in the basal plane spacing was also observed with respect to the increase in filler volume fraction, but it was too insignificant and it can be safely said that no or minimum intercalation in the composites could be observed. However, owing to the qualitative nature of X-ray peaks as well as due to better interfacial interactions in the wake of thermally stable modification and the effect of shearing forces, a decrease in the tactoid thickness and hence increase in the aspect ratio can still be expected. Figure 1(a) shows the SEM micrographs of composite containing 3 vol% of the filler fraction. A mixed morphology with single clay layers and tactoids of different thickness were observed along with bending, folding and complete misalignment of the platelets. Figure 1(b) also shows the TEM micrograph of the 3 vol% OMMT-PP composites. The thin platy tactoids could be observed which though are misoriented, but are also uniformly distributed.

Table 1 details the tensile properties of OMMT–PP nanocomposites containing different filler inorganic volume fraction. Figure 2 shows the relative tensile modulus of these composites plotted as a function of the inorganic filler volume fraction. The tensile modulus of the composites linearly increased with volume fraction with an increase of 35% at 4 vol% as compared to the pure PP. Halpin–Tsai model was used to fit the data as denoted by the solid line in Figure 2 taking $\eta = 1$, which resulted into a value of 7.46 for ζ, indicating that possibly in these nanocomposites it cannot be simply taken as twice the aspect ratio as generally used [49]. Recently, a new approach has been reported which helps to replace filler particles by stacks of filler platelets in the analysis, which is more realistic owing to the mixed morphology seen in the micrographs [40]. Different curves can be generated based on number of platelets present in the stack, when this method is applied to conventional Halpin–Tsai equation as shown in Figure 3. Relative tensile modulus for 1 and 2 vol% OMMT composites was observed to lie on the curve with 150 platelets in the stack, however, further sagging in the curve was observed with composites with higher volume fractions of the filler.

The above-mentioned analysis with Halpin–Tsai models contains inherent errors when applied to nanocomposite systems owing to the incapability of the model to consider the effect of misoriented platelets on the modulus. Figure 4(a) shows the relative tensile modulus of the OMMT–PP composites plotted against the curves representing different number of platelets in the stack when incomplete exfoliation and platelets misalignment effects were also incorporated in the Halpin–Tsai model [39]. The experimental values were observed to lie on an average in between 100 and 150 platelets in the stack. The behavior of the composites was also compared using the models suggested by Brune and Bicerano, which also was incorporated with considerations of incomplete exfoliation and misorientation [41].

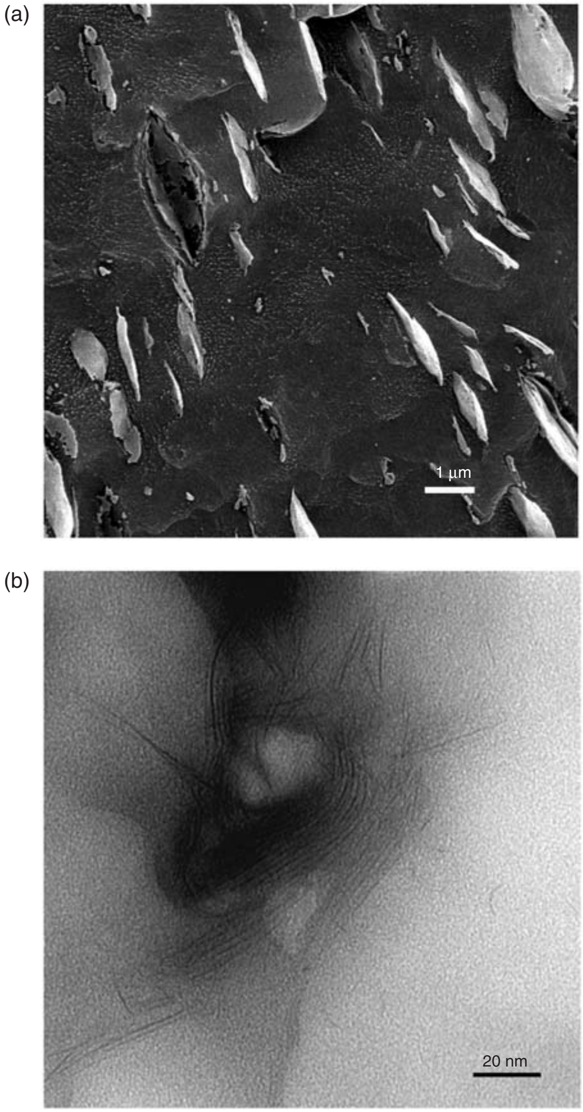

Figure 1. *(a) SEM and (b) TEM micrographs of 3 vol% OMMT–PP nanocomposites. The black lines in the TEM micrograph represent the cross-section of clay platelets.*

Figure 4(b) shows that the experimental data follows the predictions of 40–50 platelets in the stack. Though the modified models can predict the nanocomposite properties more accurately than the conventional models, however, one major limitation of these mechanical models is the assumption

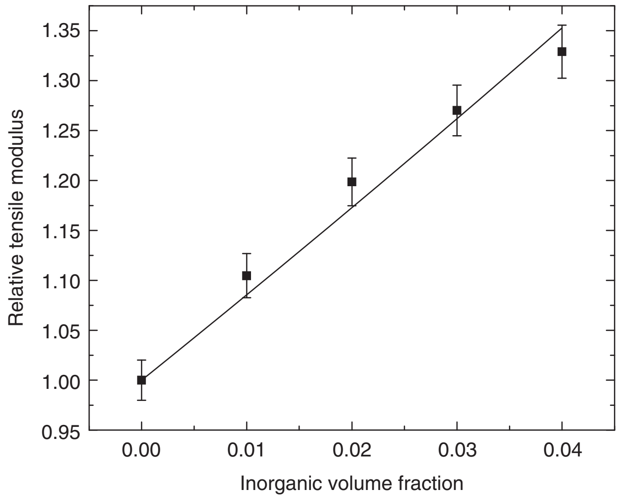

Figure 2. *Relative tensile modulus of OMMT–PP nanocomposites as a function of inorganic volume fraction. The solid line represents the fitting by using unmodified Halpin–Tsai equation.*

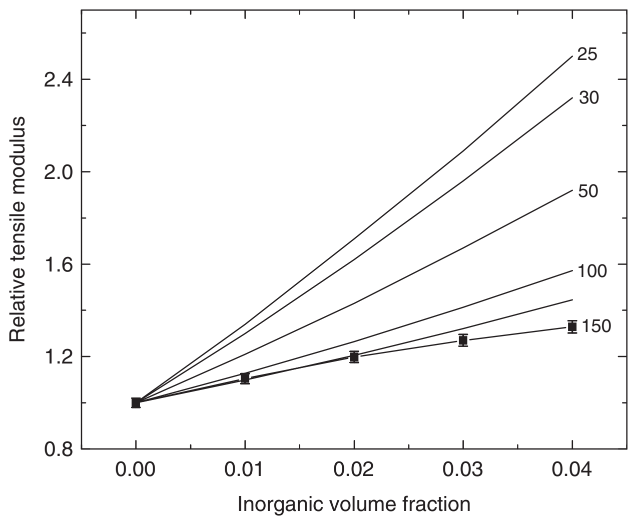

Figure 3. *Relative tensile modulus of OMMT–PP nanocomposites (■: experimental) compared with the values considering different number of platelets in the stack [39].*

of perfect adhesion at the interface. The polyolefin composites studied in the current work, really lack this adhesion, as only weak van der Waals forces can exist in the studied polymer organic monolayer systems. It is also important to note that determination of aspect ratio from the TEM micrographs can really be misleading owing to the bending and misalignment of platelets as shown in the micrographs presented in this study thus requiring a model to estimate overall average aspect ratio.

It was also of interest to model other mechanical properties of the composites with the theoretical models. It was suggested by Nielsen [50] that

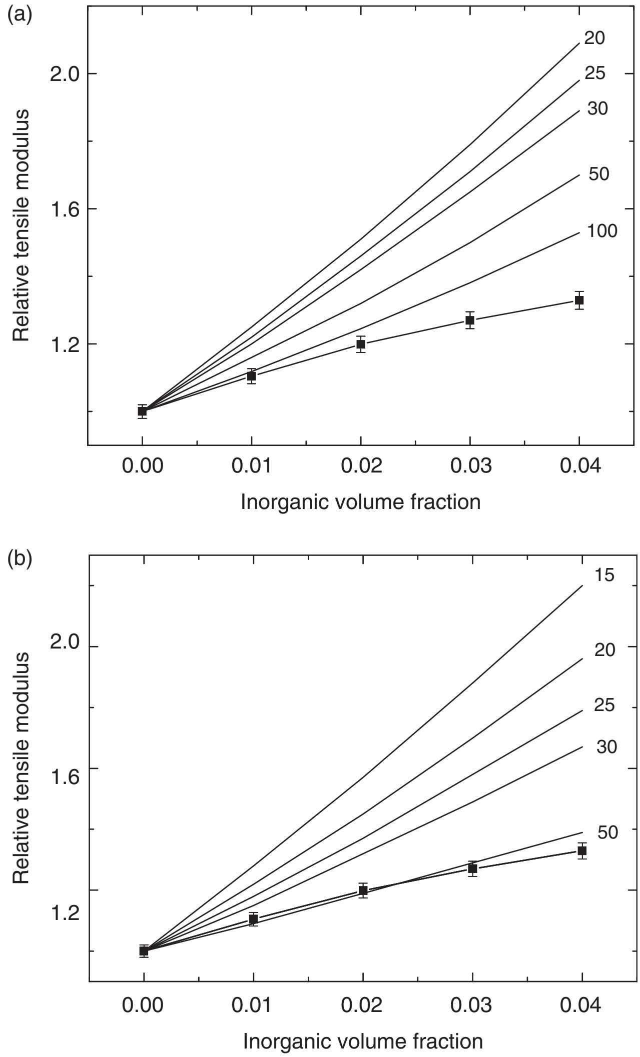

Figure 4. *a and b: relative tensile modulus of OMMT–PP nanocomposites (■: experimental) as a function of inorganic volume fraction compared with the values considering different number of platelets in the stack applying platelet misorientation models [36,40].*

strain ratio, $\varepsilon_c/\varepsilon_m$ for the polymer composites can be predicted by the simple equation as

$$\frac{\varepsilon_c}{\varepsilon_m} = 1 - \varphi_f^{1/3}$$

where ε_c and ε_m are the yield strains of the composite and matrix, respectively, and φ_f is the filler volume fraction. The model was based on the assumption that the polymer breaks at the same elongation in the filled composite as the bulk unfilled polymer does. Figure 5(a) compares the model prediction of yield strain with the experimental results plotted as a function of filler volume fraction. Both experimental and theoretical values showed a decrease in the strain with increasing volume fraction, but much lower values of relative yield strain (dotted line in Figure 5(a)) were obtained experimentally than predicted (solid line in Figure 5(a)) indicating lack of interfacial adhesion between the organic–inorganic components and the

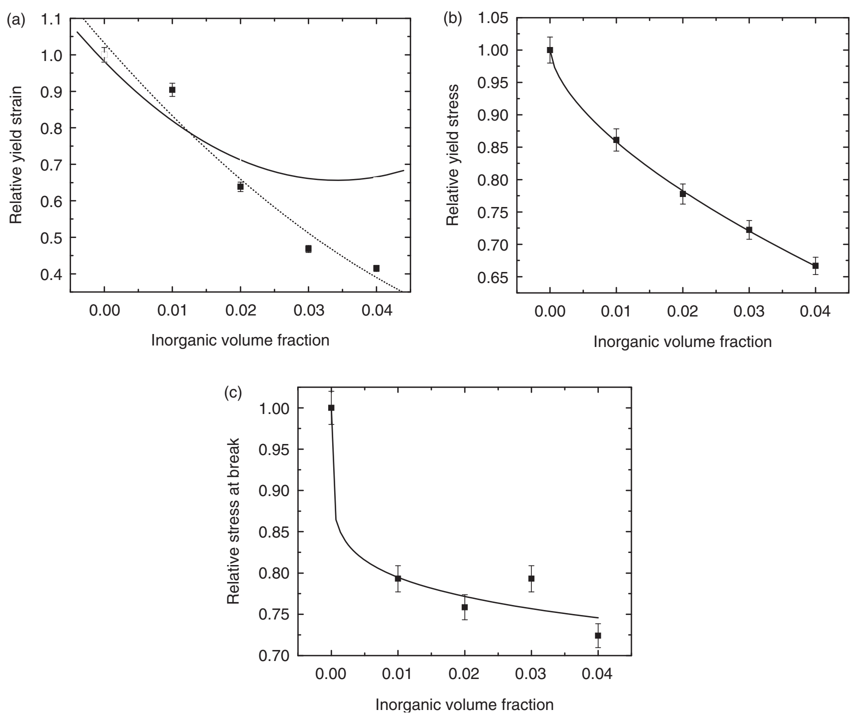

Figure 5. *(a) Relative yield strain, (b) relative yield stress, and (c) relative stress at break of the OMMT–PP nanocomposites. The solids lines represent the fitting of the experimental values with the empirical models, whereas the dotted line serves as a guide.*

strain hardening of the confined polymer. The composites also became subsequently brittle as a function of increasing inorganic volume fraction.

The yield stress and stress at break of the filled polymers was described by Nicolais and Nicodemo [51] with the following equation:

$$\frac{\sigma}{\sigma_1} = 1 - P_1\varphi^{P_2}$$

where P_1 is stress concentration related constant with a value of 1.21 for the spherical particles having no adhesion with the matrix and P_2 is geometry related constant with a value of 0.67 when the sample fails by random failure. Figure 5(b) and c detail the yield stress and stress at break properties as a function of filler volume fraction. The yield strength decayed with augmenting the filler volume fraction indicating the lack of adhesion at the interface and brittleness. Thus, it is possible that the platelets in the present case may have been only kinetically trapped, which leads to straining of the confined polymer chains. The experimental values when fitted with Nicolais and Nicodemo model yielded P_1 as 2.44 and P_2 as 0.61, thus deviating from the values obtained for the spherical particles [49]. More nonlinear decrease was observed for stress at break with filler volume fraction owing to the similar reasons and presence of tactoids. The fitting of the stress at break values in the model yielded P_1 and P_2 as 0.42 and 0.15, respectively, which shows higher deviation from the spherical particle predictions.

PP-g-MA has been commonly used as a compatibilizer in the OMMT–PP nanocomposites in order to reduce the interfacial energy thus causing more exfoliation. Three different kinds of compatibilizers were selected on the basis of chemical composition and the location of the polar groups in the polymer chain. PP-g-MA1 had a high-molecular weight as indicated by its low MFI of 5.5 g (10 min, 230°C, 2.16 kg) with MA content of 0.1 wt%, whereas PP-g-MA2 had a M_n of 3900 and had 4 wt% of MA content corresponding to 3.7 MA units per polymer chain, thus, making it high-MA compatibilizer (acid number 47 mg KOH/g of PP-g-MA). In order to analyze the effect of block copolymers on the performance of nanocomposites, PP-b-PPG (polypropylene glycol) was synthesized [44]. Figure 6 shows the chemical architecture of the synthesized copolymer. The resulting copolymer is not strictly diblock copolymer, but still can be represented as one and can be visualized as PP chains containing polar blocks as side chains instead of small MA molecules. The amount of the compatibilizer in the composites was kept low in order not to affect the mechanical and crystallization behavior of the polymer composites. A compatibilizer/OMMT weight ratio of 0.16 was used in the composites. The amount of compatibilizer was fixed to 2 wt% owing to the deterioration of mechanical properties at higher amounts of compatibilizers in an earlier reported study and 2 wt% was found to be an optimum amount [44].

The 001 basal plane spacing values of the composites carrying 2 wt% of various compatibilizers (inorganic filler volume fraction was always kept to be 3%) have been compared with the one without compatibilizer in Table 2. The WAXRD patterns have also been shown in Figure 7. The presence of basal peaks indicated that no full exfoliation has taken place. Apart from that, the increase in the basal plane spacing is also minimal indicating a very less amount of compatibilizer could actually intercalate the clay interlayers. One reason for this may be the initial lower basal plane spacing of the filler requiring higher mechanical shear to delaminate or to intercalate as compared to the dioctadecyldimethylammonium modified montmorillonite. As the increase in the *d*-spacing is minimal, it may also indicate that the mechanical shear exerted in the compounder may not have been optimum. However, the *d*-spacing increased with increasing the polarity of the compatibilizer. PP-b-PPG with maximum polarity showed an increase of 0.3 nm as compared to the value of 2.24 for OMMT. As said before, as the peak intensity and width are sensitive to many factors thus, the diffractograms cannot accurately quantify the extent of exfoliation and the exact quantification of the effect of compatibilizers can only be achieved through the analysis of resulting composite properties. Figure 8 also shows the TEM micrograph

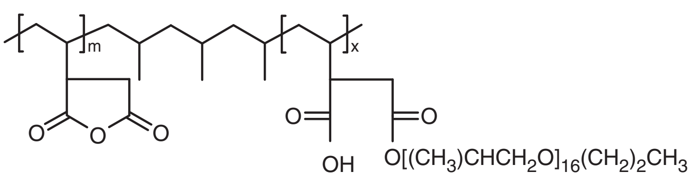

Figure 6. *Chemical structure of PP-b-PPG synthesized by the reaction of PP-g-MA2 with PP glycol monobutyl ether.*

Table 2. ***d-spacing values of pure matrices and 3 vol% OMMT–PP nanocomposites with and without 2 wt% compatibilizer.***

Compatibilizer (2 wt%)	*d*-spacing (nm)
Pure PP	–
PP + PP-g-MA2	–
No compatibilizer	2.29
PP-g-MA1	2.28
PP-g-MA2	2.31
PP-b-PPG	2.51

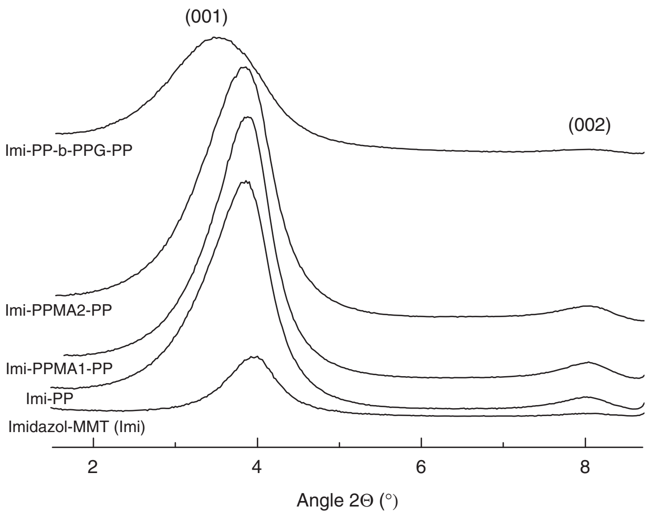

Figure 7. *X-ray diffractograms of imidazolium treated clay and its 3 vol% composites with and without 2 wt% of compatibilizer.*

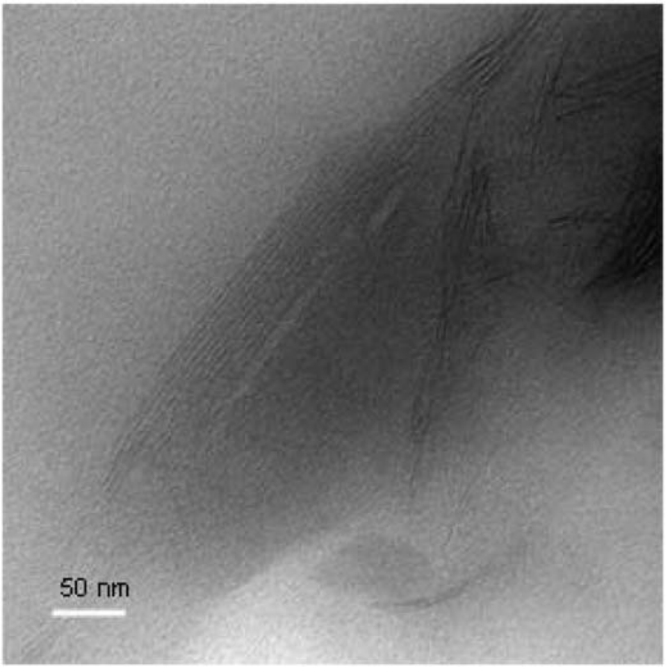

Figure 8. *TEM micrograph of polypropylene clay nanocomposites with 2 wt% of PP-b-PPG compatibilizer.*

of the PP composites with 2 wt% of PP-b-PPG compatibilizer. One can see that the tactoid thickness has been reduced as compared to the TEM micrograph of the composites without compatibilizer. The decrease in tactoid thickness represents increase in aspect ratio of the filler, thus can also be called as increased delamination, though delamination of every platelet to nanometer scale is still not achieved.

Mechanical properties of the composites with and without compatibilizer along with pure PP have been detailed in Table 3. All the compatibilizers increased the tensile modulus of the composites as compared to the composite without compatibilizer owing to increased extent of exfoliation on addition of compatibilizers. Figure 9(a) also shows the correlation between the relative modulus and the *d*-spacing of OMMT in these composites. The modulus was observed to be roughly unchanged with respect to *d*-spacing indicating only exfoliated layers are responsible for the improvement in modulus. Also the plasticization effects generally associated with the compatibilizers may limit the further improvement of the modulus. Increase in the yield strain of the composites with compatibilizer as compared to the composite without compatibilizer also indicated weak plasticization of the polymer. The strain also was observed to marginally increase with increasing *d*-spacing and the polarity of the comaptibilizer. Yield stress and the stress at break were also observed to be almost unchanged as the composite without compatibilizer indicating the presence of little brittleness and non-optimum interfacial interactions. Relative yield stress was also observed to be independent of *d*-spacing, while the break stress was observed to decrease with increase in *d*-spacing (Figure 9(a) and (b)). The presence of tactoids, which are not efficient enough for load transfer can be a reason for this decrease. Only 2 wt% compatibilizer was used in this study as the properties were observed to deteriorate when the amount

Table 3. Tensile properties of pure matrices and 3 vol% OMMT–PP nanocomposites with and without 2 wt% compatibilizer.

Compatibilizer (2 wt%)	Tensile modulus[a] (MPa)	Yield stress[b] (MPa)	Yield strain[c] (%)	Stress at break[d] (MPa)
Pure PP	1510	36	9.4	29
PP + PP-g-MA2	1463	33	10.5	36
No compatibilizer	1918	26	4.4	23
PP-g-MA1	2039	26	5.5	24
PP-g-MA2	2023	27	5.8	25
PP-b-PPG	1993	26	5.5	22

Notes: [a]Relative probable error 5%.
[b]Relative probable error 2%.
[c]Relative probable error 5%.
[d]Relative probable error 15%.

of compatibilizer was increased beyond 2 wt% in a similar study on PP nanocomposites [44].

Although the addition of only 2 wt% of the compatibilizers had a significant effect on the mechanical properties of the composites, the calorimetric properties were observed to be affected minimally as described in Table 4. The onset and peak melting temperatures were observed to be unchanged. PP-g-MA2 and PP-b-PPG were observed to reduce the peak crystallization temperature as compared to pure PP, whereas marginal advancement in the onset of crystallization was observed for PP-g-MA1. Degree of crystallization values calculated from the enthalpy of melting, however, were fairly constant. Therefore, the effect on the composite properties due to the addition of the compatibilizers can be safely attributed to the organic inorganic interactions and compatibilizing forces rather than changes in degree of crystallinity.

The oxygen permeation coefficients through the nanocomposite films with different compatibilizers have been listed in Table 5 along with of OMMT–PP composite without compatibilizer, pure PP and a blend of PP with 2 wt/% PP-g-MA2. The permeation through the composite films containing compatibilizer decreased as compared to the pure PP but the decrease was either lesser or same as the composite without any compatibilizer. Though further decrease in the oxygen permeation is expected on the addition of compatibilizer owing to increased exfoliation, however opposite phenomenon was observed. Similar results have also been observed for the composites with dimethyldioctadecyl ammonium treated montmorillonite [44]. As the blend of PP and the compatibilizer seem to have no effect on the permeation of PP, the compatibility of the treated clay with the

Table 4. Calorimetric properties of pure matrices and 3 vol% OMMT–PP nanocomposites with and without 2 wt% compatibilizer.

Compatibilizer (2 wt%)	$T^a_{m,onset}$ (°C)	T^b_m (°C)	ΔH_mpolymer (J/g)	Crystallinity[c] (X_c)	$T^d_{c,onset}$ (°C)	T^e_c (°C)
Pure PP	152	162	96	0.58	114	112
PP + PP-g-MA2	152	165	94	0.57	112	106
No compatibilizer	153	163	97	0.59	115	111
PP-g-MA1	153	162	95	0.58	120	114
PP-g-MA2	152	163	93	0.56	114	107
PP-b-PPG	151	164	92	0.56	114	108

Notes: [a]Onset melting temperature.
[b]Peak melt temperature.
[c]Degree of crystallinity calculated using ΔH of 100% crystalline PP = 165 J/g [52,53].
[d]Onset crystallization temperature.
[e]Peak crystallization temperature.

compatibilizer molecules can be a very serious issue. Micro voids or increase in free volume generated at the interface because of the incompatibility of these two phases can lead to an increase in the permeation, though the clay is more exfoliated or the effect of exfoliation can be counterbalanced leading to no decrease or increase in the permeation [6]. This is the reason that an improvement in mechanical properties is observed after the addition of even a small amount of compatibilizer, however, a deterioration of interface sensitive micro properties like gas permeation is observed. This phenomenon can be visualized as a balance of two factors i.e., enhancement in diffusion owing to increase in voids or mismatching and decrease in permeant diffusion owing to generation of more tortuous path by the exfoliated platelets.

It was also of interest to determine the thermal behavior of the OMMT–PP nanocomposites synthesized with and without 2 wt% of compatibilizer. As the compatibilizers have significantly lower molecular weight than the matrix polymer, therefore, the thermal performance of the combined system may be affected thus requiring quantifying the effect. Figure 10(a) shows the TGA thermograms of nanocomposites mixed with and without 2 wt% of different compatibilizers (inorganic volume fraction is always fixed at 3 vol%). As is clearly evident that the various curves are indistinguishable and the thermal behavior of the composites with and without the added compatibilizers is the same thus confirming that the thermal behavior of the system is not affected on addition of compatibilizers. Figure 10(b) also provides further comparison of the thermal behavior of pure polymer (I), polymer and 2 wt% of PP-g-MA2 (II), imidazolium modified clay (III), and polymer composite with 3 vol% of filler and 2 wt% of PP-g-MA2 (IV). It is clear from the TGA thermogram of the composite that synergism in between the organic and organic parts of the composites leads to better thermal properties than any of the components.

Table 5. Oxygen permeation values of pure matrices and 3 vol% OMMT–PP nanocomposites with and without 2 wt% compatibilizer.

Compatibilizer (2 wt%)	Permeability coefficient (cm^3 $\mu m/m^2$ day mm Hg)
Pure PP	89
PP + PP-g-MA2	83
No compatibilizer	57
PP-g-MA1	69
PP-g-MA2	61
PP-b-PPG	78

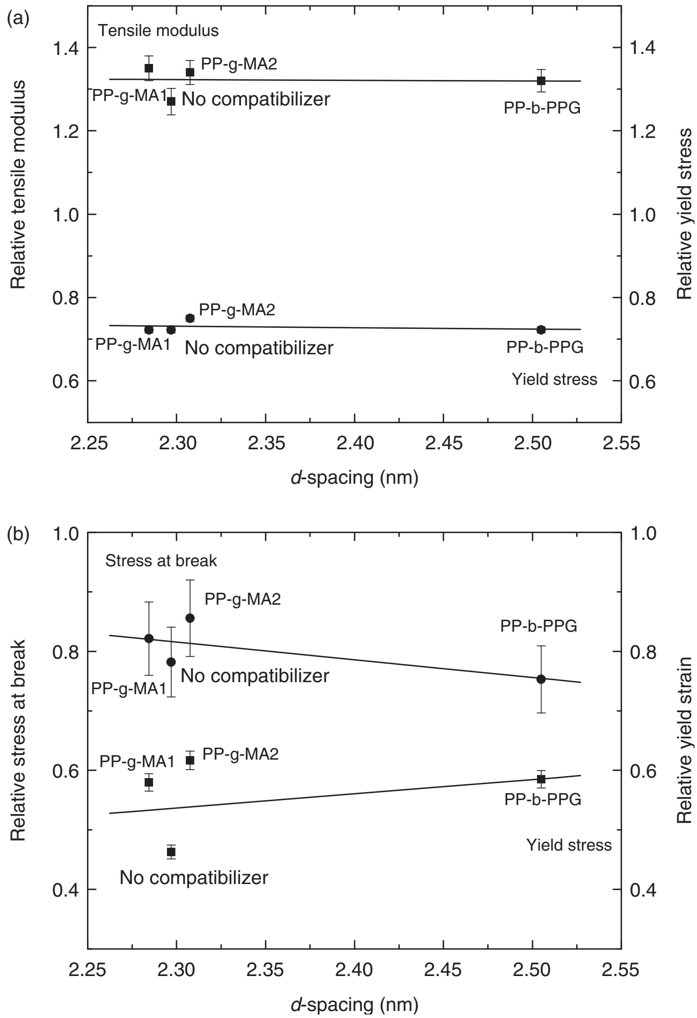

Figure 9. *Relative tensile modulus and yield stress and (b) relative stress at break and yield strain of 3 vol% OMMT–PP nanocomposites with and without 2 wt% compatibilizer.*

CONCLUSIONS

PP nanocomposites employing montmorillonite modified with thermally stable imidazolium modification as compared to conventional ammonium modification were synthesized. The mechanical properties of the nanocomposites could be modeled with Halpin–Tsai models and more recent models incorporating other considerations for the correct prediction of

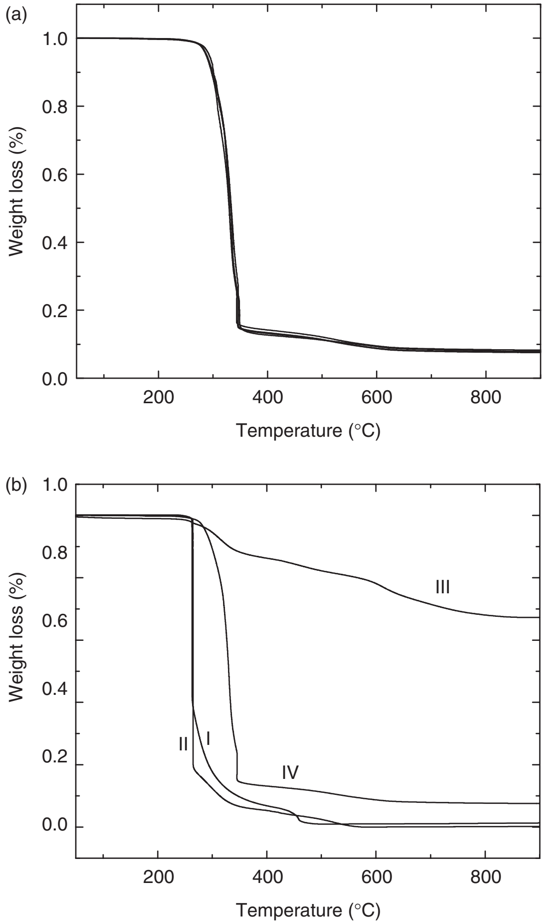

Figure 10. *(a) TGA thermograms of 3 vol% OMMT nanocomposites with and without 2 wt% compatibilizer and (b) TGA thermograms of pure PP (I), PP-g-MA2 (II), OMMT (III) and 3 vol% OMMT-polypropylene composite with 2 wt% of PP-g-MA2 compatibilizer (IV).*

nanocomposites properties like misorientation, incomplete exfoliation etc. A partial delamination was achieved in OMMT–PP nanocomposites even without the use of compatibilizer and overall a mixed morphology consisting of clay tactoids of varying thicknesses represented the microstructure of the composites. Addition of small amounts of compatibilizer further improved the delamination of the filler. Tensile modulus of the compatibilized nanocomposites increased as compared to the composites generated without compatibilizer though a slight plasticization of the matrix was also observed. The oxygen permeation through the compatibilized composites did not show any improvement as compared to the non-compatibilized composites owing to the competing phenomena of increase in permeation due to interfacial mismatching and increase in free volume with decrease in permeation due to tortuous permeant pathway generated by the exfoliated platelets. The addition of compatibilizer did not affect the crystallization behavior of PP and the thermal behavior of the compatibilized composites represented the synergistic behavior of the individual components thus indicating the thermal stability of the system in the presence of compatibilizer.

ACKNOWLEDGMENTS

Financial support from the Swiss National Science Foundation (SNF) and TOP NANO 21 of the ETH board is greatly acknowledged.

REFERENCES

1. Usuki, A., Kojima, Y., Kawasumi, M., Okada, A., Fukushima, Y., Kurauchi, T. and Kamigaito, O. (1993). Synthesis of Nylon 6-Clay Hybrid, *Journal of Materials Research*, **8**: 1179–1184.
2. LeBaron, P.C., Wang, Z. and Pinavaia, T.J. (1999). Polymer-Layered Silicate Nanocomposites: An Overview, *Applied Clay Science*, **15**: 11–29.
3. Giannelis, E.P. (1996). Polymer Layered Silicate Nanocomposites, *Advanced Materials*, **8**: 29–35.
4. Alexandre, M. and Dubois, P.H. (2000). Polymer-Layered Silicate Nanocomposites: Preparation, Properties and Uses of a New Class of Materials, *Materials Science and Engineering R*, **28**: 1–63.
5. Gilman, J.W., Jackson, C.L., Morgan, A.B., Harris, R., Manias, E., Giannelis, E.P., Wuthenow, M., Hilton, D. and Phillips, S.H. (2000). Flammability Properties of Polymer-Layered Silicate Nanocomposites. Polypropylene and Polystyrene Nanocomposites, *Chemistry of Materials*, **12**: 1866–1873.
6. Osman, M.A., Mittal, V., Morbidelli, M. and Suter, U.W. (2003). Polyurethane Adhesive Nanocomposites as Gas Permeation Barrier, *Macromolecules*, **36**: 9851–9858.
7. Bailey, S.W. (ed.) (1984). Classification and Structures of the Micas, In: *Reviews in Mineralogy*, Virginia Polytechnic Institute and State University, Blacksburg, VA, pp. 1–60.
8. Bailey, S.W. (1980). Structures of Layer Silicates, In: Brindley, G.W. and Brown, G. (eds), *Crystal Structure of Clay Minerals and Their X-ray Identification*, pp. 1–124, Mineralogical Society, London.
9. Theng, B.K.G. (1974). *The Chemistry of Clay-Organic Reactions*, Adam Hilger, London.
10. Lagaly, G. and Beneke, K. (1991). Intercalation and Exchange Reactions of Clay Minerals and Non-clay Layer Compounds, *Colloid and Polymer Science*, **269**: 1198–1211.
11. Pukanszky, B. (1995). Particulate Filled Polypropylene: Structure and Properties, In: Karger-Kocsis, J. (ed.), *Polypropylene Structure, Blends and Composites*, Vol. 3, pp. 1–70, Chapman and Hall, London.
12. Jancar, J. (1999). *Mineral Fillers in Thermoplastics, Advances in Polymer Science*, Vol. 139, Springer, Berlin.

13. Radosta, J.A. and Trivedi, N.C. (1987). Talc, In: Katz, H.S. and Milevski, J.V. (eds), *Handbook of Fillers for Plastics*, pp. 216–231, Van Nostrand Reinhold Company, New York.
14. Xie, W., Gao, Z., Pan, W.P., Hunter, D., Singh, A. and Vaia, R. (2001). Thermal Degradation Chemistry of Alkyl Quaternary Ammonium Montmorillonite, *Chemistry of Materials*, **13**: 2979–2990.
15. Gilman, J.W. (1999). Flammability and Thermal Stability Studies of Polymer Layered-silicate (clay) Nanocomposites, *Applied Clay Science*, **15**: 31–49.
16. VanderHart, D.L., Asano, A. and Gilman, J.W. (2001). NMR Measurements Related to Clay-dispersion Quality and Organic-modifier Stability in Nylon-6/Clay Nanocomposites, *Macromolecules*, **34**: 3819–3822.
17. Fornes, T.D., Yoon, P.J., Keskkula, H. and Paul, D.R. (2001). Nylon 6 Nanocomposites: The Effect of Matrix Molecular Weight, *Polymer*, **42**: 9929–9940.
18. Vander Hart, D.L., Asano, A. and Gilman, J.W. (2001). Solid-state NMR Investigation of Paramagnetic Nylon-6/Clay Nanocomposites. 2. Measurement of Clay Dispersion, Crystal Stratification, and Stability of Organic Modifiers, *Chemistry of Materials*, **13**: 3796–3809.
19. Gilman, J.W., Morgan, A., Harris Jr, R., Jackson, C. and Hunter, D. (2000). Phenolic Cyanate Ester Clay Nanocomposites: Effect of Ammonium Ion Structure Flammability and Nano-dispersion, *Polymeric Materials Science and Engineering, Preprints*, **82**: 276–277.
20. Rossi, G.B., Beaucage, G., Dang, T.D. and Vaia, R.A. (2002). Bottom-up Synthesis of Polymer Nanocomposites and Molecular Composites: Ionic Exchange with PMMA Latex, *Nano Letters*, **2**: 319–323.
21. Mark, J.E. (1996). Ceramic-reinforced Polymers and Polymer-modified Ceramics, *Polymer Engineering and Science*, **36**: 2905–2920.
22. Yasue, K., Tamura, T., Katahira, S. and Watanabe, M. (1995). Reinforced Polymamide Resin Composition and Process for Producing the Same, US Patent 5,414,042.
23. Awad, W.H., Gilman, J.W., Nyden, M., Harris Jr, R.H., Sutto, T.E., Callahan, J., Trulove, P.C., DeLong, H.C. and Fox, D.M. (2004). Thermal Degradation Studies of Alkyl-imidazolium Salts and Their Application in Nanocomposites, *Thermochimica Acta*, **409**: 3–11.
24. Zhu, J., Morgan, A.B., Lamelas, F.J. and Wilkie, C.A. (2001). Fire Properties of Polystyrene-clay Nanocomposites, *Chemistry of Materials*, **13**: 3774–3780.
25. Kawasumi, M., Hasegawa, N., Kato, M., Usuki, A. and Okada, A. (1997). Preparation and Mechanical Properties of Polypropylene-clay Hybrids, *Macromolecules*, **30**: 6333–6338.
26. Hasegawa, N., Kawasumi, M., Kato, M., Usuki, A. and Okada, A. (1998). Preparation and Mechanical Properties of Polypropylene-clay Hybrids Using a Maleic Anhydride-modified Polypropylene Oligomer, *Journal of Applied Polymer Science*, **67**: 87–92.
27. Svoboda, P., Zeng, C., Wang, H., Lee, L.J. and Tomasko, D.L. (2002). Morphology and Mechanical Properties of Polypropylene/Organoclay Nanocomposites, *Journal of Applied Polymer Science*, **85**: 1562–1570.
28. Lopez, D.C., Picazo, O., Merino, J.C. and Pastor, J.M. (2003). Polypropylene–Clay Nanocomposites: Effect of Compatibilizing Agents on Clay Dispersion, *European Polymer Journal*, **39**: 945–950.
29. Wang, Y., Chen, F.B., Li, Y.C. and Wu, K.C. (2004). Melt Processing of Polypropylene/Clay Nanocomposites Modified with Maleated Polypropylene Compatibilizers, *Composites Part B – Engineering*, **35**: 111–124.
30. Lertwimolnun, W. and Vergnes, B. (2005). Influence of Compatibilizer and Processing Conditions on the Dispersion of Nanoclay in a Polypropylene Matrix, *Polymer*, **46**: 3462–3471.
31. Chiu, F.C., Lai, S.M., Chen, J.W. and Chu, P.S. (2004). Combined Effects of Clay Modifications and Compatibilizers on the Formation and Physical Properties of Melt-mixed Polypropylene/Clay Nanocomposites, *Journal of Polymer Science, Part B: Polymer Physics*, **42**: 4139–4150.

32. Xu, W., Liang, G., Wang, W., Tang, S., He, P. and Pan, W.P. (2003). PP-PP-g-MA-Org-MMT Nanocomposites. 1. Intercalation Behavior and Microstructure, *Journal of Applied Polymer Science*, **88**: 3225–3231.
33. Narh, K.A., Bhaskar, A., Tortorela, N. and Beatty, C.L. (2003). ANTEC 2003, 3717.
34. Osman, M.A., Rupp, J.E.P. and Suter, U.W. (2005). Effect of Non-ionic Surfactants on the Exfoliation and Properties of Polyethylene-Layered Silicate Nanocomposites, *Polymer*, **46**: 8202–8209.
35. Kerner, E.H. (1956). The Elastic and Thermo-Elastic Properties of Composite Media, *Proceedings of the Physical Society*, **B69**: 808–813.
36. Halpin, J.C. (1992). *Primer on Composite Materials Analysis*, Technomic, Lancaster.
37. Hashin, Z. and Shtrikman, S. (1963). A Variational Approach to the Theory of the Elastic Behavior of Multiphase Materials, *Journal of the Mechanics and Physics of Solids*, **11**: 127–140.
38. Halpin, J.C. (1969). Stiffness and Expansion Estimates for Oriented Short Fiber Composites, *Journal of Composite Materials*, **3**: 732–734.
39. van Es, M., Xiqiao, F., van Turnhout, J. and van der Giessen, E. (2001). Comparing Polymer-Clay Nanocomposites with Conventional Composites Using Composite Modeling, In: Al-Malaika, S., Golovoy, A.W. and Wilkie, C.A. (eds), *Specialty Polymer Additives: Principles and Application*, pp. 391–414, Blackwell Science, CA Melden, MA.
40. Fornes, T.D. and Paul, D.R. (2003). Modeling Properties of Nylon 6/Clay Nanocomposites Using Composite Theories, *Polymer*, **44**: 4993–5013.
41. Brune, D.A. and Bicerano, J. (2002). Micromechanics of Nanocomposites: Comparison of Tensile and Compressive Elastic Moduli, and Prediction of Effects of Incomplete Exfoliation and Imperfect Alignment on Modulus, *Polymer*, **43**: 369–387.
42. Osman, M.A. and Suter, U.W. (2000). Determination of the Cation-exchange Capacity of Muscovite Mica, *Journal of Colloid and Interface Science*, **224**: 112–115.
43. Mittal, V. (2007). Gas Permeation and Mechanical Properties of Polypropylene Nanocomposites with Thermally-stable Imidazolium Clay, *European Polymer Journal*, **43**: 3727–3736.
44. Mittal, V. (2008). Mechanical and Gas Permeation Properties of Compatibilized Polypropylene-layered Silicate Nanocomposites, *Journal of Applied Polymer Science*, **107**: 1350–1361.
45. Osman, M.A., Mittal, V. and Suter, U.W. (2007). Poly(propylene)-layered Silicate Nanocomposites: Gas Permeation Properties and Clay Exfoliation, *Macromolecular Chemistry and Physics*, **208**: 68–75.
46. Mittal, V. (2007). Polypropylene-layered Silicate Nanocomposites: Filler Matrix Interactions and Mechanical Properties, *Journal of Thermoplastic Composite Materials*, **20**: 575–599.
47. Osman, M.A. and Atallah, A. (2004). High-density Polyethylene Micro- and Nanocomposites: Effect of Particle Shape, Size and Surface Treatment on Polymer Crystallinity and Gas Permeability, *Macromolecular Rapid Communications*, **25**: 1540–1544.
48. Osman, M.A. and Rupp, J.E.P. (2005). Interfacial Interactions and Properties of Polyethylene-layered Silicate Nanocomposites, *Macromolecular Rapid Communications*, **26**: 880–884.
49. Osman, M.A., Rupp, J.E.P. and Suter, U.W. (2005). Tensile Properties of Polyethalene-Layered Silicate Nanocomposites, *Polymer*, **46**: 1653–1660.
50. Nielsen, L.E. (1966). Simple Theory of Stress-Strain Properties of Filled Polymers, *Journal of Applied Polymer Science*, **10**: 97–103.
51. Nicolais, L. and Nicodemo, L. (1973). Strength of Particulate Composite, *Polymer Engineering and Science*, **13**: 469.
52. Fatou, J.G. (1971). Melting Temperature and Enthalpy of Isotactic Polypropylene, *European Polymer Journal*, **7**: 1057–1064.
53. Wunderlich, B. (1980). *Macromolecular Physics*, Vol. 3, Academic Press, New York.